

Ejected from home: C/1980 E1 (Bowell) and C/2024 L5 (ATLAS)

R. de la Fuente Marcos¹, C. de la Fuente Marcos², and S. J. Aarseth³

¹AEGORA Research Group, Facultad de Ciencias Matemáticas, Universidad Complutense de Madrid, Ciudad Universitaria, E-28040 Madrid, Spain

²Universidad Complutense de Madrid, Ciudad Universitaria, E-28040 Madrid, Spain

³Institute of Astronomy, University of Cambridge, Madingley Road, Cambridge CB3 0HA, UK

Received 19 August 2024 / Accepted 25 September 2024

ABSTRACT

Context. Natural interstellar objects do not form isolated in deep space, but escape their natal planetary systems. Early removal from their home star systems via close flybys with still-forming planets could be the dominant ejection mechanism. However, dynamically evolved planetary systems such as the Solar System may also be a significant source of natural interstellar objects.

Aims. We studied the dynamical evolution of two unusual Solar System hyperbolic comets, C/1980 E1 (Bowell) and C/2024 L5 (ATLAS), to investigate the circumstances that led them to reach moderate Solar System excess hyperbolic speeds.

Methods. We used N -body simulations and statistical analyses to explore the planetary encounters that led to the ejection of C/1980 E1 and C/2024 L5, and studied their pre- and post-encounter trajectories.

Results. We confirm that C/1980 E1 reached its present path into interstellar space after an encounter with Jupiter at 0.23 au on December 9, 1980. C/2024 L5 was scattered out of the Solar System following a flyby to Saturn at 0.003 au on January 24, 2022. Integrations backward in time show that C/1980 E1 came from the inner Oort cloud but C/2024 L5 could be a former retrograde, inactive Centaur. The receding velocities of C/1980 E1 and C/2024 L5 when entering interstellar space will be 3.8 and 2.8 km s⁻¹, moving towards Aries and Triangulum, respectively.

Conclusions. Our results for two comets ejected from the Solar System indicate that dynamically evolved planetary systems can be effective sources of interstellar objects and provide constraints on their velocity distribution.

Key words. comets: general – comets: individual: C/1980 E1 (Bowell) – comets: individual: C/2024 L5 (ATLAS) – methods: data analysis – methods: numerical – celestial mechanics

1. Introduction

Natural and artificial objects can reach interstellar space from their home planetary systems via the gravitational slingshot mechanism by which, under the right conditions, a small body, moving past a more massive one also in motion, can be accelerated via conservation of momentum and energy (see, e.g., Saslaw et al. 1974). For natural objects, this process is far more probable within dynamically young environs such as the star-forming regions where star clusters and stellar associations are born (see, e.g., Bally 2006; Davies 2015; Parker 2020). Inside them, scattering by young, still-forming planets (see, e.g., Fernandez 1978; Brassier et al. 2006) and passing stars (see, e.g., Portegies Zwart et al. 2018; Pfalzner et al. 2021) may trigger bursts of ejected debris. In this context, natural interstellar objects are mostly a by-product of the violent and chaotic processes that lead to the formation of planetary systems (see, e.g., Stern 1990).

By the time planet formation is over, essentially < 100 Myr, large amounts of the material originally present in a protoplanetary disk may already have been ejected (see, e.g., fig. 1 in Pfalzner & Bannister 2019; Pfalzner et al. 2021); a fraction of this debris could be in the form of interstellar objects of sizes similar to those of present-day asteroids and comets in the Solar System (Sekanina 1976; McGlynn & Chapman 1989). However, the end of planet formation and the settling of planetary systems and their host stars as part of the field population do not suppress

the gravitational slingshot mechanism but merely reduce its effectiveness and efficiency. Most field stars remain in the main sequence for > 1 Gyr and the continuous operation of the gravitational slingshot mechanism over extended periods of time, albeit at a much lower efficiency, can still generate an unfaltering stream of interstellar objects.

Here, we study the dynamical evolution of two rare Solar System hyperbolic comets, C/1980 E1 (Bowell) and C/2024 L5 (ATLAS), to investigate the circumstances that led them to reach moderate excess hyperbolic speeds with respect to the barycenter of the Solar System. This paper is organized as follows. In Sect. 2, we provide information on the input data and methods used in our numerical investigation. In Sect. 3, we study the present dynamical status, and the past and future evolution of comet C/1980 E1; those of comet C/2024 L5 are considered in Sect. 4. We discuss our dynamical results in Sect. 5 and summarize our conclusions in Sect. 6.

2. Data and tools

To investigate the dynamical evolution of the objects under study here, we analyzed results from direct N -body simulations. To carry out these calculations, we used orbit determinations and other relevant Solar System data (as of September 19, 2024) from the Jet Propulsion Laboratory's (JPL) Small-Body Database (SBDB)¹ provided by the Solar System Dynam-

Send offprint requests to: R. de la Fuente Marcos, e-mail: rauldefuentemarcos@ucm.es

¹ https://ssd.jpl.nasa.gov/tools/sbdb_lookup.html#/

ics Group (SSDG, Giorgini 2011, 2015).² and input data from JPL's HORIZONS³ on-line solar system data and ephemeris computation service, updated with the DE440/441 solution (Park et al. 2021). Data was retrieved from SBDB using the PYTHON package ASTROQUERY (Ginsburg et al. 2019) and its HORIZONSCLASS⁴ and SBDBCLASS⁵ classes.

The N -body simulations needed to investigate the evolution of the objects discussed in this paper were carried out using a direct N -body code described by Aarseth (2003) that is publicly available from the web site of the Institute of Astronomy of the University of Cambridge.⁶ This software makes use of the Hermite numerical integration scheme developed by Makino (1991). Our calculations do not include the Galactic potential as they consist of integrations on comparatively short timescales (1 Myr), while the Sun takes ~ 220 Myr to complete one revolution around the center of the Galaxy. The orbit determinations in Table 1 did not require non-gravitational terms to fit the data; therefore, any contribution due to asymmetric outgassing is probably a second order effect in these cases and the impact of non-gravitational forces could be safely neglected and was not included in the calculations. Additional technical details, relevant results from this code as well as comparisons with results from other codes used for validation were presented in de la Fuente Marcos & de la Fuente Marcos (2012). Our physical model included the perturbations by the eight major planets, the Moon, the barycenter of the Pluto-Charon system, and the three largest asteroids, Ceres, Pallas, and Vesta. Initial conditions for the comets under study here were generated by applying the Monte Carlo using the Covariance Matrix (MCCM) methodology described in de la Fuente Marcos & de la Fuente Marcos (2015). The relevant covariance matrices were retrieved from JPL's SBDB by using the SBDBCLASS class.

Figures were produced using Matplotlib (Hunter 2007) and statistical tools provided by NumPy (van der Walt et al. 2011; Harris et al. 2020). Histograms have statistically meaningful bin sizes and show the probability density so that the area under the histogram integrates to 1. The bin width was computed using the Freedman-Diaconis rule (Freedman & Diaconis 1981). The Galactic space velocities were computed as described by Johnson & Soderblom (1987) using the values of the relevant parameters provided by Schönrich et al. (2010).

3. Ejected by Jupiter: C/1980 E1 (Bowell)

Comet C/1980 E1 (Bowell) — also known as Comet Bowell 1982 I = 1980b — was first imaged by E. L. G. Bowell on February 11, 1980, while observing at the Anderson Mesa Station of the Lowell Observatory in Arizona (Bowell et al. 1980a) with the 33-cm astrograph (the same instrument used to discover Pluto 50 years before), although the actual discovery image was acquired on March 13, 1980, with the same telescope. When first observed, it was moving inwards at 7.24 au from the Sun and was described as diffuse, with no obvious condensation. The comet reached perihelion on March 12, 1982, and it was last observed on December 30, 1986, from the Steward Observatory in Kitt Peak by the Spacewatch project 0.9-m telescope, when it was located at 13.92 au from the Sun, heading for the outskirts of the Solar System.

The orbit determination of C/1980 E1 available from JPL's SBDB and computed on April 15, 2021 (see Table 1), is based on 187 data points for a data-arc span of 2514 d, and is referred to epoch JD 2444972.5 that is the instant $t = 0$ for these calculations. With a current value of the heliocentric orbital eccentricity, e , of 1.0577 and a barycentric one of 1.0477 — fourth only to those of 1I/2017 U1 ('Oumuamua), the first known interstellar object (see, e.g., Williams 2017; Meech et al. 2017; Hainaut et al. 2018; 'Oumuamua ISSI Team et al. 2019), 2I/Borisov, the first *bona fide* interstellar comet (see, e.g., de León et al. 2019; Fitzsimmons et al. 2019; Jewitt & Luu 2019; Guzik et al. 2020), and the poorly-known comet C/1954 O1 (Vozarova) — it has the lowest value of the orbital inclination ($1^{\circ}66'17''$) among those of known nearly-parabolic ($e \sim 1$) to hyperbolic ($e > 1$) small bodies. The cause of its present high eccentricity is well understood — it was the result of a close encounter with Jupiter on December 9, 1980 (see, e.g., Bowell et al. 1980b; Buffoni et al. 1982; Branham 2013) — but its actual origin and pre-discovery orbital evolution are still unclear.

Soon after discovery, it was argued that C/1980 E1 could be a first-time visitor from the Oort cloud (Seki et al. 1980), recently perturbed by a stellar flyby or perhaps an interstellar comet (Hasegawa et al. 1981). Engelhardt et al. (2017) pointed out that the orbital properties of C/1980 E1 are compatible with those of interstellar objects although bordering those of slightly perturbed Oort cloud comets, but it is still widely assumed that the origin of this comet is in the Oort cloud (see, e.g., Królikowska & Dybczyński 2017; Hui 2018), although no detailed calculations have been published since the latest public orbit determination was announced. With a data-arc span of 6.88 yr and being hyperbolic at nearly the 5990σ level (barycentric), a detailed numerical exploration using the latest data may help to confirm the dynamical status of C/1980 E1 prior to discovery and its close planetary encounter.

We explored the close encounter of C/1980 E1 with Jupiter by performing 10^3 N -body simulations based on the MCCM methodology as pointed out in Sect. 2. The median and 16th and 84th percentiles of the minimum approach distance to Jupiter during the flyby matched their average value and its standard deviation, as expected from the small uncertainties of the orbit determination (see Table 1). The minimum approach distance was 0.228122 ± 0.000006 au, the Hill radius of Jupiter is 0.338 au, and the calendar date for this flyby was 1980-Dec-09 11:06; HORIZONS gives a value of 1980-Dec-09 11:03 \pm 00:09 and a nominal minimum approach distance to Jupiter of 0.22841 au. Table 2 shows the pre-encounter orbit of C/1980 E1 as reconstructed from the results of our calculations. It corresponds to a near-parabolic comet with an orbital eccentricity (median and 16th and 84th percentiles) of $0.999961^{+0.000008}_{-0.000007}$. Although C/1980 E1 now follows a hyperbolic path, its orbit prior to encountering Jupiter was bound and similar to those of thousands of known Solar System comets. Our analysis of short-term integrations assigns exactly zero probability to the hypothesis of having a hyperbolic orbit right before its encounter with Jupiter.

However, its minimum orbit intersection distance (MOID) with Jupiter was sufficiently small to have led to close flybys with Jupiter in previous passages through the inner Solar System. Within this dynamical context, C/1980 E1 might be an old comet, a new one recently dislodged from the Oort cloud or, less likely, a low-relative-velocity, temporary capture from interstellar space — under the right circumstances, the gravitational slingshot mechanism can lead to a capture instead of an ejection. The analysis of the evolution into the past of 10^3 control orbits of C/1980 E1 generated using an MCCM process shows

² <https://ssd.jpl.nasa.gov/>

³ <https://ssd.jpl.nasa.gov/?horizons>

⁴ <https://astroquery.readthedocs.io/en/latest/jplhorizons/jplhorizons.html>

⁵ <https://astroquery.readthedocs.io/en/latest/jplsbdb/jplsbdb.html>

⁶ <http://www.ast.cam.ac.uk/~sverre/web/pages/nbody.htm>

Table 1. Keplerian orbital elements of comets C/1980 E1 (Bowell) and C/2024 L5 (ATLAS).

Parameter	C/1980 E1 (Bowell)		C/2024 L5 (ATLAS)	
	heliocentric	barycentric	heliocentric	barycentric
Perihelion, q (au)	= 3.363940±0.000003	3.355370	3.4320±0.0006	3.4400
Eccentricity, e	= 1.057733±0.000008	1.047673	1.0375±0.0003	1.0352
Inclination, i (°)	= 1.66174±0.00006	1.66170	166.5729±0.0003	166.6027
Longitude of the ascending node, Ω (°)	= 114.557±0.002	114.5621	139.166±0.003	139.158
Argument of perihelion, ω (°)	= 135.083±0.002	135.1432	290.52±0.02	290.49
Mean anomaly, M (°)	= 359.84868±0.00003	359.88609	359.730±0.003	359.755
MOID with Jupiter (au)	= 0.0108537	—	0.00499388	—
Total magnitude, M_1 (mag)	= 5.8±1.0	—	6.6±0.5	—

Notes. Values include the 1σ uncertainty. The orbit of C/1980 E1 (solution date, April 15, 2021, 23:29:29 PST) is referred to epoch JD 2444972.5, which corresponds to 00:00 on 1982 January 3 TDB (Barycentric Dynamical Time, J2000.0 ecliptic and equinox) and it is based on 187 observations with a data-arc span of 2514 d. The orbit of C/2024 L5 (solution date, September 11, 2024, 13:42:21 PDT) is referred to epoch JD 2460504.5, which corresponds to 00:00 on 2024 July 13 TDB and it is based on 215 observations with a data-arc span of 82 d. Source: JPL’s SBDB.

Table 2. Computed pre-planetary encounter Keplerian orbital elements of comets C/1980 E1 (Bowell) and C/2024 L5 (ATLAS).

Parameter	C/1980 E1 (Bowell)	C/2024 L5 (ATLAS)
Perihelion, q (au)	= 3.179958±0.000005	8.0 ^{+0.5} _{-0.4}
Eccentricity, e	= 0.999962±0.000008	0.70±0.02
Inclination, i (°)	= 1.77204±0.00010	153±2
Longitude of the ascending node, Ω (°)	= 120.638±0.002	137.1±0.2
Argument of perihelion, ω (°)	= 134.485±0.002	240 ⁺⁶ ₋₈

Notes. The pre-planetary encounter orbit estimate of C/1980 E1 includes mean values and 1σ uncertainties and it is the result of 10^3 N -body calculations back in time as described in the text. The one of C/2024 L5 shows medians and 16th and 84th percentiles from 10^4 simulations.

that 1 Myr ago, C/1980 E1 was located at 28792^{+1288}_{-1272} au from the Sun, moving with a radial velocity of 0.027 ± 0.012 km s⁻¹ (see Fig. 1). Valtonen & Innanen (1982) showed that a relative velocity exceeding 0.5 km s⁻¹ when near the Hill radius of the Solar System is required to become interstellar. An interstellar origin, as a recent capture, is therefore strongly rejected.

On the other hand, from a similar set of calculations forward in time, at 3.8595 ± 0.0003 pc from the Sun and 1.0 Myr into the future, C/1980 E1 will be receding from us (see Fig. 2) at 3.7695 ± 0.0003 km s⁻¹ towards (apex) $\alpha=03^{\text{h}} 16^{\text{m}} 34.9^{\text{s}}$, $\delta=+16^{\circ} 37' 00.1''$ ($49^{\circ}1454\pm 0^{\circ}0012$, $+16^{\circ}6167\pm 0^{\circ}0003$) in the constellation of Aries with Galactic coordinates $l=166^{\circ}00$, $b=-33^{\circ}85$ (see Fig. 3, top panel), and ecliptic coordinates $\lambda=51^{\circ}17$, $\beta=-01^{\circ}49$. The components of its heliocentric Galactic velocity will be $(U, V, W)=(-3.0392\pm 0.0002$, $+0.7532\pm 0.0001$, $-2.0988\pm 0.0002)$ km s⁻¹ (see Fig. 3, bottom panels).

4. Ejected by Saturn: C/2024 L5 (ATLAS)

Comet C/2024 L5 (ATLAS) was discovered on June 14, 2024, as A117uUD, by the Asteroid Terrestrial-impact Last Alert System (ATLAS, Tonry et al. 2018) observing with the unit located in the Sutherland plateau in South Africa (Rhemann et al. 2024; Green 2024). The orbit determination of C/2024 L5 available from JPL’s SBDB and computed on September 11, 2024 (see Table 1), is based on 215 data points for a data-arc span of 82 d, and is referred to epoch JD 2460504.5 that is the instant $t = 0$ for these calculations. With a current value of the heliocentric orbital eccentricity, e , of 1.0375 and a barycentric one of 1.0352, C/2024 L5 follows C/1980 E1 (Bowell) as the known small body with the fifth highest value of e . Based on early data, S. Nakano (Green 2024) and de la Fuente Marcos & de la Fuente Marcos (2024) concluded that the comet had experienced a very close

encounter with Saturn on January 24, 2024, leading to its present hyperbolic trajectory ($\sim 126\sigma$ level, barycentric) from an initially bound ($e < 1$) but retrograde ($i > 90^{\circ}$) orbit.

Using the latest public orbit determination in Table 1, we studied the close encounter of C/2024 L5 with Saturn by performing 10^4 N -body simulations based on the MCCM methodology (see Sect. 2). Our results are summarized in Figs. 4 and 5. The comet experienced an encounter with Saturn at very close range in 2022 and this makes the reconstruction of its pre-encounter path difficult. The top panel in Fig. 4 displays the minimum approach distance (color-coded) to Saturn during the flyby as a function of the (q, e) values for each synthetic orbit. The median and 16th and 84th percentiles, 0.0027 ± 0.0003 au, indicate that the encounter took place well inside the Hill radius of Saturn, 0.412 au, but not inside the Roche radius (see, e.g., Crida & Charnoz 2014) of the planet, 0.000932 au (see Fig. 4, middle panel). Therefore, it is highly unlikely that its current level of cometary activity could be the result of any flyby-induced fragmentation event. Consistently, the comet was inactive by mid-2023 (S. Deen 2024, private communication). The histogram of calendar dates for this flyby in Fig. 4, bottom panel, shows a median of 2022-Jan-24 04:25, HORIZONS gives 2022-Jan-24 02:51±07:43 and a nominal minimum approach distance to Saturn of 0.00269 au.

As for the dynamical nature of this comet prior to its encounter with Saturn, Fig. 5 shows the distribution of the resulting pre-flyby eccentricity; the top panel displays the color-coded values as a function of (q, e) ; the bottom panel presents the histogram of pre-encounter eccentricities with median and 16th and 84th percentiles of 0.70 ± 0.02 . The probability of C/2024 L5 having a pre-encounter orbital eccentricity equal to or higher than that of ‘Oumuamua, 1.20113, or 2I/Borisov, 3.35648, is 0.0; the probability of having a non-hyperbolic pre-encounter trajectory is 1.0. Our best estimate for the orbit of C/2024 L5 prior to

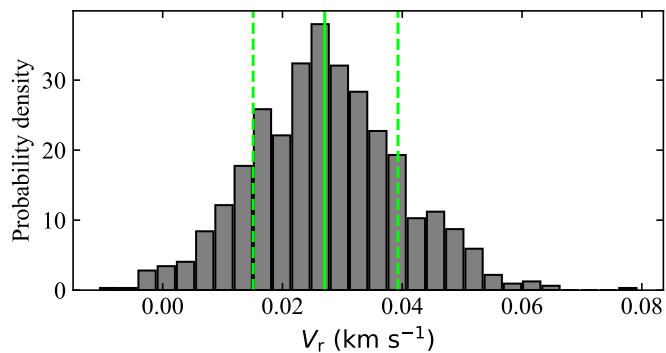
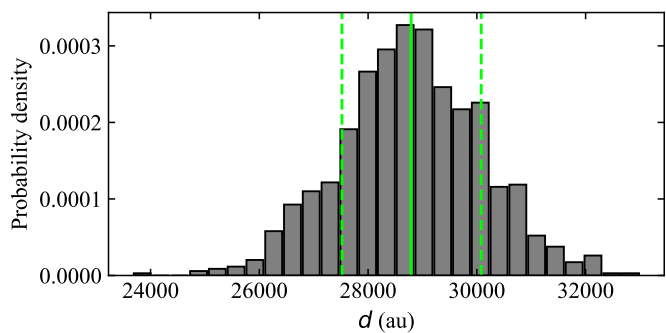


Fig. 1. Range or distance and range rate or radial velocity of C/1980 E1 (Bowell), 1.0 Myr before its close encounter with Jupiter. *Top panel:* Distribution of distances at the end of the simulations, 28792^{+1288}_{-1272} au. *Bottom panel:* Distribution of radial velocities at the end of the calculations, 0.027 ± 0.012 km s⁻¹. Distributions resulting from the evolution of 10^3 control orbits. The median is displayed as a continuous vertical green line, the 16th and 84th percentiles as dashed lines.

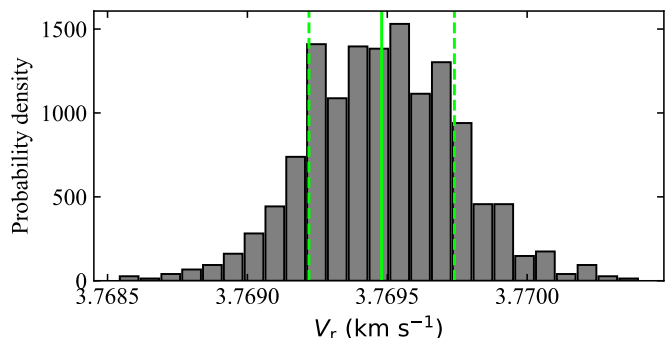


Fig. 2. Receding velocity of C/1980 E1 (Bowell) after escaping the Solar System. Distribution resulting from the evolution of 10^3 control orbits for 1.0 Myr. The median is displayed as a continuous vertical green line, the 16th and 84th percentiles as dashed lines, 3.7695 ± 0.0003 km s⁻¹.

its encounter with Saturn is shown in Table 2 and in Figs. 5 and 6.

Having low MOID with both Jupiter and Saturn, this object may have had a very chaotic dynamical past. The analysis of the evolution of 10^3 control orbits of C/2024 L5 generated using an MCCM process and integrated backward in time shows that 1.0 Myr ago, C/2024 L5 was located at 36^{+14}_{-12} au from the Sun, so around the trans-Neptunian region, moving with a radial velocity of $0.00^{+0.08}_{-0.09}$ km s⁻¹ (see Fig. 7). An interstellar origin (as a recent capture) is strongly rejected, the probability of capture from interstellar space is $0.00^{+0.02}_{-0.00}$ for integrations 1.0 Myr into the past (several sets).

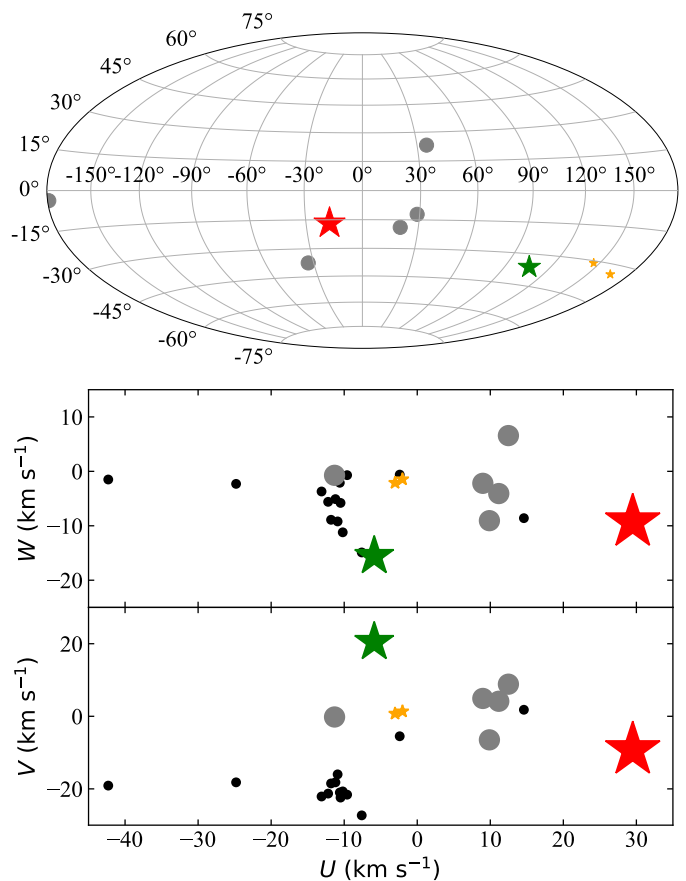


Fig. 3. Apex and velocity of known natural and artificial interstellar objects. *Top panel:* Location of the apex of each interstellar object in Galactic coordinates. Comet 2I/Borisov is shown as a red star and 1I/2017 U1 (‘Oumuamua) is displayed in green. From left to right, C/2024 L5 (ATLAS) and C/1980 E1 (Bowell) are displayed as orange stars, Pioneer 10, Voyager 2, New Horizons, Pioneer 11, and Voyager 1 are shown as grey circles. Coordinates are displayed in a Hammer-Aitoff equal-area projection. *Bottom panels:* Heliocentric Galactic velocity components at apex of the same objects and velocities of stellar groups within 100 pc from the Sun in black.

Regarding its future, the analysis of the evolution of a similar set of 10^3 control orbits shows that all of them lead to escaping from the Solar System with a velocity of $2.836^{+0.013}_{-0.012}$ km s⁻¹ after 1.0 Myr (see Fig. 8), when the comet will be located 2.906 ± 0.013 pc from the Solar System receding from us towards $\alpha=02^{\text{h}} 21^{\text{m}} 14^{\text{s}}$, $\delta=+28^{\circ} 00' 00''$ ($35^{\circ} 31 \pm 0^{\circ} 09$, $+28^{\circ} 00 \pm 0^{\circ} 03$) in the constellation of Triangulum with Galactic coordinates $l=146^{\circ} 05$, $b=-30^{\circ} 81$, and ecliptic coordinates $\lambda=42^{\circ} 27$, $\beta=+13^{\circ} 16$. The components of its heliocentric Galactic velocity will be $(U, V, W)=(-2.022 \pm 0.009, +1.358 \pm 0.006, -1.453 \pm 0.007)$ km s⁻¹ (see Fig. 3, bottom panels).

5. Discussion

Our numerical results strongly reject an extrasolar origin for C/1980 E1 (Bowell), as a recent capture; for C/2024 L5 (ATLAS), it emerges as a low-probability setting. Here, we focus on the probable dynamical classes of their parent bodies. Being part of a certain dynamical class at any given time does not necessarily imply that a small body was formed in the region of the Solar System that is hosting that class. A dramatic example of this fact is in the Manx comets that are made of materials ori-

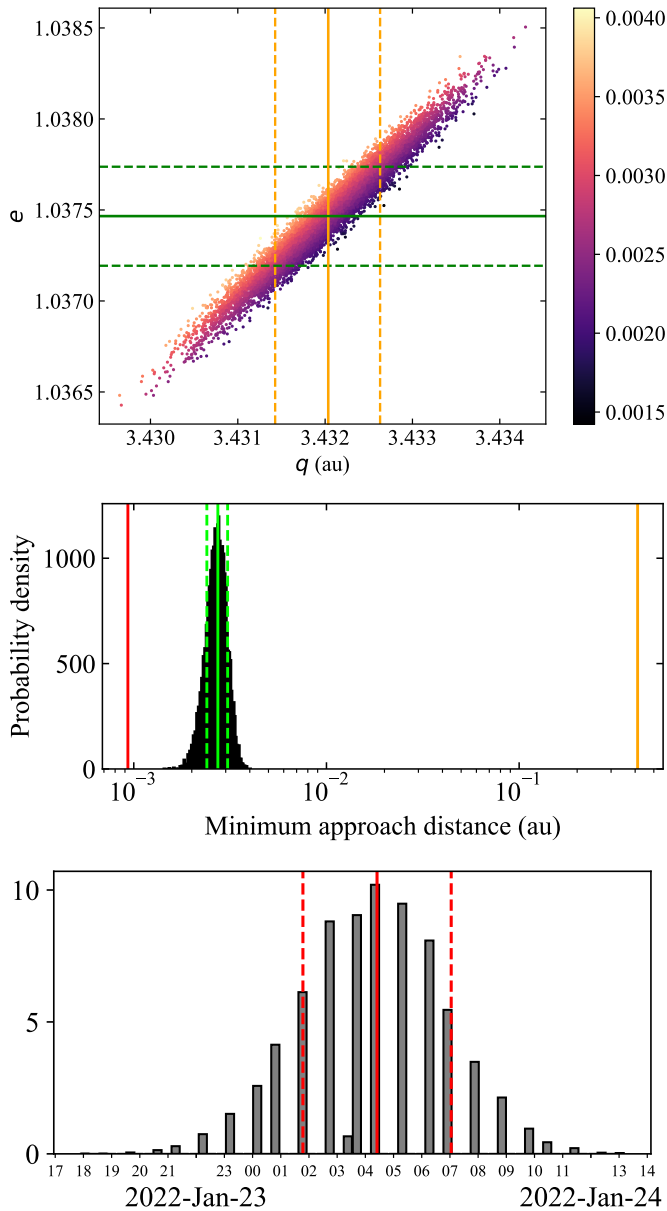


Fig. 4. Close encounter of C/2024 L5 (ATLAS) with Saturn. *Top panel:* Minimum approach distance (color-coded) as a function of the values of (q, e) at $t = 0$. Median values are shown as continuous (green for e , orange for q) lines, 16th and 84th percentiles as dashed lines. *Middle panel:* Distribution of minimum approach distances, the median and 16th and 84th percentiles, 0.0027 ± 0.0003 au, are shown in green, the Hill radius of Saturn is 0.412 au (in orange), and the Roche radius is 0.000932 au (in red). *Bottom panel:* Distribution of calendar dates for the flyby, the median and 16th and 84th percentiles (in red) are 2022-Jan-24 04:25±02:38. The output cadence (time resolution) in our calculations was 0.877 h.

inally formed in the inner Solar System although their present-day trajectories come from the Oort cloud (Meech et al. 2016). Unfortunately, the numerical reconstruction of the past orbital evolution of objects in highly-chaotic paths has limitations. The conservation of the Tisserand invariant can be used to identify some of the original parameters of such orbits (Namouni 2022, 2024). Spectroscopic observations (or in situ analyses via robotic missions) can provide reliable information on the region where the material that constitutes the small body was originally processed (see, e.g., Pieters & McFadden 1994).

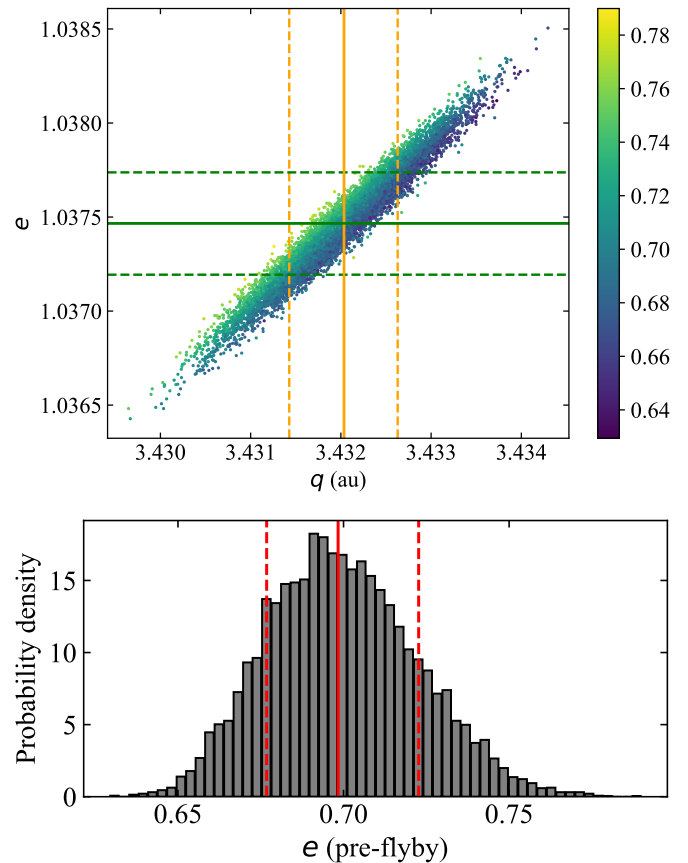


Fig. 5. Distribution of the pre-flyby eccentricity of C/2024 L5 (ATLAS). *Top panel:* Values of the pre-flyby eccentricity (color-coded) as a function of the input values of (q, e) at $t = 0$. Median values are shown as continuous (green for e , orange for q) lines, 16th and 84th percentiles as dashed lines. *Bottom panel:* Distribution of the computed pre-flyby eccentricity. The median is displayed as a continuous red line, 16th and 84th percentiles as dashed lines, 0.70 ± 0.02 .

On the other hand, Pfalzner et al. (2021) argued that the ejection velocity of interstellar objects produced by planet scattering is $\sim 4\text{--}8$ km s $^{-1}$. Our calculations suggests either a smaller lower limit for the ejection velocity after planetary encounters in evolved planetary systems, or a lower median or most probable value, as the receding velocities of C/1980 E1 and C/2024 L5 when entering interstellar space will be 3.8 and 2.8 km s $^{-1}$, respectively.

In addition, here we provide a basic analysis of a different aspect of the problem of production of interstellar objects, that of the artificial ones. Over four decades ago, when the Pioneer 10 probe reached the escape velocity, the Solar System started producing artificial interstellar objects, 4.5682 Gyr after its own formation (Bouvier & Wadhwa 2010). Alien civilizations as technologically advanced as ours are expected to produce artificial interstellar objects as well (Bracewell 1960; Sagan 1963). Our deep space probes escape the Solar System after one or more gravity-assist maneuvers, which are precisely planned applications of the gravitational slingshot mechanism (see, e.g., Silver 1968; Flandro 1968).

5.1. An inner Oort cloud origin for C/1980 E1

Our calculations (see Sect.3) place the origin of C/1980 E1 (Bowell) in the torus-shaped inner Oort cloud or Hills cloud

(Hills 1981; Levison et al. 2001), not the spherical classical Oort cloud whose outer edge might be 10^5 au from the Sun (Oort 1950). Inner Oort cloud candidate members have been discovered during the last two decades (Brown et al. 2004; Trujillo & Sheppard 2014; Sheppard et al. 2019). On the other hand, it has a spectrum consistent with an origin in the Solar System (Jewitt et al. 1982). Based on the available evidence, the hypothesis of an origin in interstellar space (as a recent capture) for this comet can be discarded.

5.2. A Centaur origin for C/2024 L5 (ATLAS)

As for the origin of C/2024 L5 (ATLAS), our calculations (see Sect.4 and Table 2) strongly suggest a Solar System provenance. However, JPL's SBDB includes no objects with values of q , e and i within the ranges shown in Table 2. When no constraint on the value of i is considered, we find one entry in the database, 2017 GY₈, a prograde Centaur — Centaurs are objects with orbits between those of Jupiter and Neptune ($5.5 \text{ au} < a < 30.1 \text{ au}$, a is the semimajor axis) and $i < 90^\circ$. Tiscareno & Malhotra (2003) found that nearly two thirds of the objects in Centaur orbits are expected to be eventually ejected into interstellar space.

Just outside the orbital domain outlined in Table 2, we find 2017 UX₅₁ with $q=7.61 \text{ au}$, $e=0.75$, and $i=90^\circ 45'$. This dynamical context and our own numerical results strongly suggest that, prior to its close planetary encounter with Saturn, C/2024 L5 was in a very unstable, retrograde trajectory similar to those of retrograde Centaurs. Volk & Malhotra (2013) argued that retrograde Centaurs are unlikely to come from the trans-Neptunian or Kuiper belt. The analysis of the past orbital evolution of known retrograde Centaurs in de la Fuente Marcos & de la Fuente Marcos (2014) concluded that they may come from the Oort cloud but the existence of a closer, previously unknown reservoir cannot be ruled out. Namouni & Morais (2020) argued for an interstellar origin of the high-inclination Centaurs, but as early captures that took place during the early stages of the formation of the Solar System. This scenario is consistent with other studies that argue for the presence of a significant fraction of extrasolar debris — originally captured from the surroundings of the nascent Solar System — in the present-day Oort cloud (see, e.g., Levison et al. 2010; Portegies Zwart et al. 2021). Fernández et al. (2018) found that retrograde Centaurs do not exhibit cometary activity and that their dynamical lifetimes are comparatively long. Li et al. (2019) pointed out that under certain conditions prograde Centaurs may turn retrograde and vice versa. Such orbital flips can be triggered by the von Zeipel–Lidov–Kozai mechanism (von Zeipel 1910; Lidov 1962; Kozai 1962; Ito & Ohtsuka 2019) via a secular resonance with, e.g., Jupiter (de la Fuente Marcos et al. 2015). This dynamical pathway has been explored by Kankiewicz (2020) for 2017 UX₅₁. However, an orbital flip for C/2024 L5 is not favored by our 1.0 Myr integrations into the past as all the control orbits remain retrograde. An interstellar origin as a recent capture seems improbable. Future astrometric and spectroscopic observations may help to confirm its source region. This comet will reach perihelion on March 10, 2025.

5.3. Leaving the Solar System: Natural versus artificial

We have also placed artificial materials in hyperbolic trajectories — the Pioneer 10 and 11 (Dyal 1993), Voyager 1 and 2 (Stone 1993), and New Horizons (Weaver et al. 2010) deep space probes, and secondary hardware from these missions such as

rocket upper stages — which may eventually be observed by extraterrestrial intelligences. II/2017 U1, 2I/Borisov, C/1980 E1 (Bowell), C/2024 L5 (ATLAS), and the five deep space probes are on their way out of the Solar System and they are not coming back. For completeness, we compare here the direction that these objects travel with respect to the Sun or apex, and also their barycentric excess hyperbolic speeds and heliocentric Galactic velocities. By studying the properties of apexes and velocities, we might be able to understand what separates natural intruders from artificial ones, dynamically. For this section, we have performed integrations forward in time for 10^5 yr of the nominal orbits of the five space probes using the latest JPL's SBDB data. Our computations neglect the possible existence of anomalous accelerations (see, e.g., Anderson et al. 1998). Our calculations are updated versions of the ones in Rudd et al. (1997) and Bailer-Jones & Farnocchia (2019).

The apex of Pioneer 10 is located towards $\alpha = 5^{\text{h}} 33^{\text{m}} 40^{\text{s}}$ and $\delta = +26^\circ 13' 1''$, in Taurus. Our calculations place the probe at 1.16 pc from the Sun receding from us at 11.4 km s^{-1} . The components of its Galactic velocity will be then $(U, V, W)=(-11.32, -0.19, -0.73) \text{ km s}^{-1}$. For Pioneer 11, we found $\alpha = 19^{\text{h}} 27^{\text{m}} 18^{\text{s}}$ and $\delta = -9^\circ 13' 16''$, in Aquila, 1.07 pc, 10.5 km s^{-1} , and $(U, V, W)=(8.98, 4.92, -2.20) \text{ km s}^{-1}$. For Voyager 1, we obtained $\alpha = 17^{\text{h}} 31^{\text{m}} 30^{\text{s}}$ and $\delta = +12^\circ 19' 2''$, in Ophiuchus, 1.70 pc, 16.7 km s^{-1} , and $(U, V, W)=(12.48, 8.85, 6.57) \text{ km s}^{-1}$. For Voyager 2, we found $\alpha = 21^{\text{h}} 5^{\text{m}} 3^{\text{s}}$ and $\delta = -67^\circ 32' 29''$, in Pavo, 1.52 pc, 14.9 km s^{-1} , and $(U, V, W)=(9.88, -6.49, -9.06) \text{ km s}^{-1}$. If its current trajectory does not change significantly, New Horizons will have $\alpha = 19^{\text{h}} 38^{\text{m}} 54^{\text{s}}$ and $\delta = -19^\circ 23' 23''$, in Sagittarius, 1.28 pc, 12.6 km s^{-1} , and $(U, V, W)=(11.16, 4.14, -4.08) \text{ km s}^{-1}$. For 'Oumuamua, we found $\alpha = 23^{\text{h}} 51^{\text{m}} 24^{\text{s}}$ and $\delta = +24^\circ 44' 59''$, in Pegasus, 2.69 pc, 26.4 km s^{-1} , and $(U, V, W)=(-5.89, 20.47, -15.56) \text{ km s}^{-1}$. The corresponding values for 2I/Borisov from de León et al. (2020) are $\alpha = 18^{\text{h}} 21^{\text{m}} 39^{\text{s}}$ and $\delta = -51^\circ 58' 37''$, in Telescopium, 1.65 pc, 32.28 km s^{-1} , and $(U, V, W)=(29.50, -9.23, -9.30) \text{ km s}^{-1}$.

The apexes of C/1980 E1 (Bowell) and C/2024 L5 (ATLAS) are located towards the same region of the sky (Fig. 3, top panel) and away from those of 2I/Borisov and the probes. The future kinematics of C/1980 E1, C/2024 L5, and the probes is not too different from that of stellar groups within 100 pc from the Sun as in table 1 of Mamajek (2016) (Fig. 3, bottom panels). On the other hand and as pointed out above, the receding velocities of C/1980 E1 and C/2024 L5 when entering interstellar space will be 3.8 and 2.8 km s^{-1} , respectively; in sharp contrast, those of interstellar probes will be significantly higher as shown above.

6. Conclusions

The Solar System can actively produce interstellar objects (see, e.g., de la Fuente Marcos et al. 2018). Before 2024, only one such object was known, C/1980 E1 (Bowell). Here, we studied its orbital evolution together with that of a recently discovered dynamical analog, C/2024 L5 (ATLAS), using direct N -body simulations and statistical analyses to explore the planetary encounters that led to their ejection from the Solar System, and their pre- and post-encounter trajectories. Our conclusions can be summarized as follows.

1. We confirm that C/1980 E1 reached its current path into interstellar space after an encounter with Jupiter at 0.23 au on December 9, 1980.
2. We find that C/1980 E1 came from the inner Oort cloud.

3. For C/1980 E1, we computed a receding velocity when entering interstellar space of 3.8 km s^{-1} , moving towards Aries.
4. We confirm that C/2024 L5 was scattered out of the Solar System following a flyby to Saturn at 0.003 au on January 24, 2022.
5. We find that, prior to its planetary encounter, C/2024 L5 was probably a retrograde, inactive Centaur.
6. The receding velocity of C/2024 L5 when entering interstellar space will be 2.8 km s^{-1} , moving towards Triangulum.

Comet C/2024 L5 joins 1I/2017 U1, 2I/Borisov, and C/1980 E1 (Bowell) in the still small sample of known natural interstellar objects, although 1I and 2I have a confirmed extrasolar provenance. Our results for two comets ejected from the Solar System confirm the widely accepted conjecture that planetary systems such as the Solar System eject bodies throughout their lives and also provide constraints on the velocity distribution of interstellar objects coming from dynamically evolved planetary systems.

Acknowledgements. We thank the anonymous referee for prompt, constructive, and helpful reports. We thank S. Deen for searching for precovery images of C/2024 L5 (ATLAS) and for comments on this particular object, and A. I. Gómez de Castro for providing access to computing facilities. Part of the calculations and the data analysis were completed on the Brigit HPC server of the ‘Universidad Complutense de Madrid’ (UCM), and we thank S. Cano Alsúa for his help during this stage. This research was partially supported by the Spanish ‘Agencia Estatal de Investigación (Ministerio de Ciencia e Innovación)’ under grant PID2020-116726RB-I00/AEI/10.13039/501100011033. In preparation of this paper, we made use of the NASA Astrophysics Data System, the ASTRO-PH e-print server, and the MPC data server.

References

- Aarseth, S. J. 2003, *Gravitational N-Body Simulations* (Cambridge: Cambridge University Press), 27
- Anderson, J. D., Laing, P. A., Lau, E. L., et al. 1998, *Phys. Rev. Lett.*, 81, 2858
- Bailer-Jones, C. A. L. & Farnocchia, D. 2019, *RNAAS*, 3, 59
- Bally, J. 2006, *Meteoritics and Planetary Science Supplement*, 41, 5391
- Bouvier, A. & Wadhwa, M. 2010, *Nat. Geosci.*, 3, 637
- Bowell, E. L. G., Fogelin, E., & Marsden, B. G. 1980a, *IAU Circ.*, 3461
- Bowell, E., Guetter, H., Herget, P., et al. 1980b, *IAU Circ.*, 3465
- Bracewell, R. N. 1960, *Nature*, 186, 670
- Branham, R. L. 2013, *Rev. Mexicana Astron. Astrofis.*, 49, 111
- Brasser, R., Duncan, M. J., & Levison, H. F. 2006, *Icarus*, 184, 59
- Brown, M. E., Trujillo, C., & Rabinowitz, D. 2004, *ApJ*, 617, 645
- Buffoni, L., Scardia, M., & Manara, A. 1982, *Moon and Planets*, 26, 311
- Crida, A. & Charnoz, S. 2014, *Complex satellite systems: a general model of formation from rings*, in *Complex Planetary Systems*, Proceedings of the International Astronomical Union, IAU Symp. 310, ed. Z. Knežević & A. Lemaître (Cambridge University Press, Cambridge), 182
- Davies, M. B. 2015, *The effects of birth environment on planetary systems, in Twenty Years of Giant Exoplanets*, ed. I. Boisse, O. Demangeon, F. Bouchy & L. Arnold (Observatoire de Haute-Provence, Institut Pythéas), 99
- de la Fuente Marcos, C. & de la Fuente Marcos, R. 2012, *MNRAS*, 427, 728
- de la Fuente Marcos, C. & de la Fuente Marcos, R. 2014, *Ap&SS*, 352, 409
- de la Fuente Marcos, C. & de la Fuente Marcos, R. 2015, *MNRAS*, 453, 1288
- de la Fuente Marcos, C. & de la Fuente Marcos, R. 2024, *RNAAS*, 8, 184
- de la Fuente Marcos, C., de la Fuente Marcos, R., & Aarseth, S. J. 2015, *MNRAS*, 446, 1867
- de la Fuente Marcos, C., de la Fuente Marcos, R., & Aarseth, S. J. 2018, *MNRAS*, 476, L1
- de León, J., Licandro, J., Serra-Ricart, M., et al. 2019, *RNAAS*, 3, 131
- de León, J., Licandro, J., de la Fuente Marcos, C., et al. 2020, *MNRAS*, 495, 2053
- Dyal, P. 1993, *Advances in Space Research*, 13, 267
- Engelhardt, T., Jedicke, R., Vereš, P., et al. 2017, *AJ*, 153, 133
- Fernandez, J. A. 1978, *Icarus*, 34, 173
- Fernández, J. A., Helal, M., & Gallardo, T. 2018, *Planet. Space Sci.*, 158, 6
- Fitzsimmons, A., Hainaut, O., Meech, K. J., et al. 2019, *ApJ*, 885, L9
- Flandro, G. A. 1968, *J. Spacecraft Rockets*, 5, 1029
- Freedman, D., & Diaconis, P. 1981, *Z. Wahrscheinlichkeitstheor. verwandte Geb.*, 57, 453
- Giorgini, J. 2011, *Summary and status of the Horizons ephemeris system*, in *Proceedings of the Journées 2010 “Systèmes de Référence Spatio-temporels”*, ed. N. Capitaine (Observatoire de Paris, France), 87
- Giorgini, J. D. 2015, *IAUGA*, 22, 2256293
- Ginsburg, A., Sipőcz, B. M., Brasseur, C. E., et al. 2019, *AJ*, 157, 98
- Green D. W. E., 2024, *Central Bureau Electronic Telegrams*, 5418
- Guzik, P., Drahus, M., Rusek, K., et al. 2020, *Nat. Astron.*, 4, 53
- Hainaut, O. R., Meech, K. J., Micheli, M., et al. 2018, *The Messenger*, 173, 13
- Harris, C. R., Millman, K. J., van der Walt, S. J., et al. 2020, *Nature*, 585, 357
- Hasegawa, I., Nakano, S., & Yabushita, S. 1981, *MNRAS*, 196, 45P
- Hills, J. G. 1981, *AJ*, 86, 1730
- Hui, M.-T. 2018, *AJ*, 156, 73
- Hunter, J. D. 2007, *Comput. Sci. Eng.*, 9, 90
- Ito, T. & Ohtsuka, K. 2019, *Monographs on Environment, Earth and Planets*, 7, 1
- Jewitt, D. & Luu, J. 2019, *ApJ*, 886, L29
- Jewitt, D. C., Soifer, B. T., Neugebauer, G., et al. 1982, *AJ*, 87, 1854
- Johnson, D. R. H., & Soderblom, D. R. 1987, *AJ*, 93, 864
- Kankiewicz, P. 2020, *Planet. Space Sci.*, 191, 105031
- Kozai, Y. 1962, *AJ*, 67, 591
- Królikowska, M. & Dybczyński, P. A. 2017, *MNRAS*, 472, 4634
- Levison, H. F., Dones, L., & Duncan, M. J. 2001, *AJ*, 121, 2253
- Levison, H. F., Duncan, M. J., Brasser, R., et al. 2010, *Science*, 329, 187
- Li, M., Huang, Y., & Gong, S. 2019, *A&A*, 630, A60
- Lidov, M. L. 1962, *Planet. Space Sci.*, 9, 719
- Makino, J. 1991, *ApJ*, 369, 200
- Mamajek, E. E. 2016, *Young Stars and Planets Near the Sun*, Proceedings of the IAU Symposium no. 314, p.21
- McGlynn, T. A. & Chapman, R. D. 1989, *ApJ*, 346, L105
- Meech, K. J., Yang, B., Kleyana, J., et al. 2016, *Science Advances*, 2, e1600038
- Meech, K. J., Weryk, R., Micheli, M., et al. 2017, *Nature*, 552, 378
- Namouni, F. 2022, *MNRAS*, 510, 276
- Namouni, F. 2024, *MNRAS*, 527, 4889
- Namouni, F. & Morais, M. H. M. 2020, *MNRAS*, 494, 2191
- Oort, J. H. 1950, *Bull. Astron. Inst. Netherlands*, 11, 91
- ‘Oumuamua ISSI Team, Bannister, M. T., Bhandare, A., et al. 2019, *Nat. Astron.*, 3, 594
- Park, R. S., Folkner, W. M., Williams, J. G., et al. 2021, *AJ*, 161, 105
- Parker, R. J. 2020, *Royal Society Open Science*, 7, 201271
- Pfalzner, S. & Bannister, M. T. 2019, *ApJ*, 874, L34
- Pfalzner, S., Aizpuru Vargas, L. L., Bhandare, A., et al. 2021, *A&A*, 651, A38
- Pieters, C. M. & McFadden, L. A. 1994, *Annual Review of Earth and Planetary Sciences*, 22, 457
- Portegies Zwart, S., Torres, S., Pelupessy, I., et al. 2018, *MNRAS*, 479, L17
- Portegies Zwart, S., Torres, S., Cai, M. X., et al. 2021, *A&A*, 652, A144
- Rhemann, G., Jaeger, M., Linder, T., et al. 2024, *Minor Planet Electronic Circulars*, 2024-O15
- Rudd, R. P., Hall, J. C., & Spradlin, G. L. 1997, *Acta Astronautica*, 40, 383
- Sagan, C. 1963, *Planet. Space Sci.*, 11, 485
- Saslaw, W. C., Valtonen, M. J., & Aarseth, S. J. 1974, *ApJ*, 190, 253
- Schönrich, R., Binney, J., & Dehnen, W. 2010, *MNRAS*, 403, 1829
- Sekanina, Z. 1976, *Icarus*, 27, 123
- Seki, T., Bowell, E., & Marsden, B. G. 1980, *IAU Circ.*, 3468
- Sheppard, S. S., Trujillo, C. A., Tholen, D. J., et al. 2019, *AJ*, 157, 139
- Silver, B. W. 1968, *Journal of Spacecraft and Rockets*, 5, 633
- Stern, S. A. 1990, *PASP*, 102, 793
- Stone, E. C. 1993, *Advances in Space Research*, 13, 301
- Tiscareno, M. S. & Malhotra, R. 2003, *AJ*, 126, 3122
- Tonry, J. L., Denneau, L., Heinze, A. N., et al. 2018, *PASP*, 130, 064505
- Trujillo, C. A. & Sheppard, S. S. 2014, *Nature*, 507, 471
- Valtonen, M. J. & Innanen, K. A. 1982, *ApJ*, 255, 307
- van der Walt, S., Colbert, S. C., & Varoquaux, G. 2011, *Comput. Sci. Eng.*, 13, 22
- Volk, K. & Malhotra, R. 2013, *Icarus*, 224, 66
- von Zeipel, H. 1910, *Astronomische Nachrichten*, 183, 345
- Weaver, H., Grundy, W., Stern, A., et al. 2010, *38th COSPAR Scientific Assembly*, 38, 3
- Williams, G. V. 2017, *Minor Planet Electronic Circulars*, 2017-V17

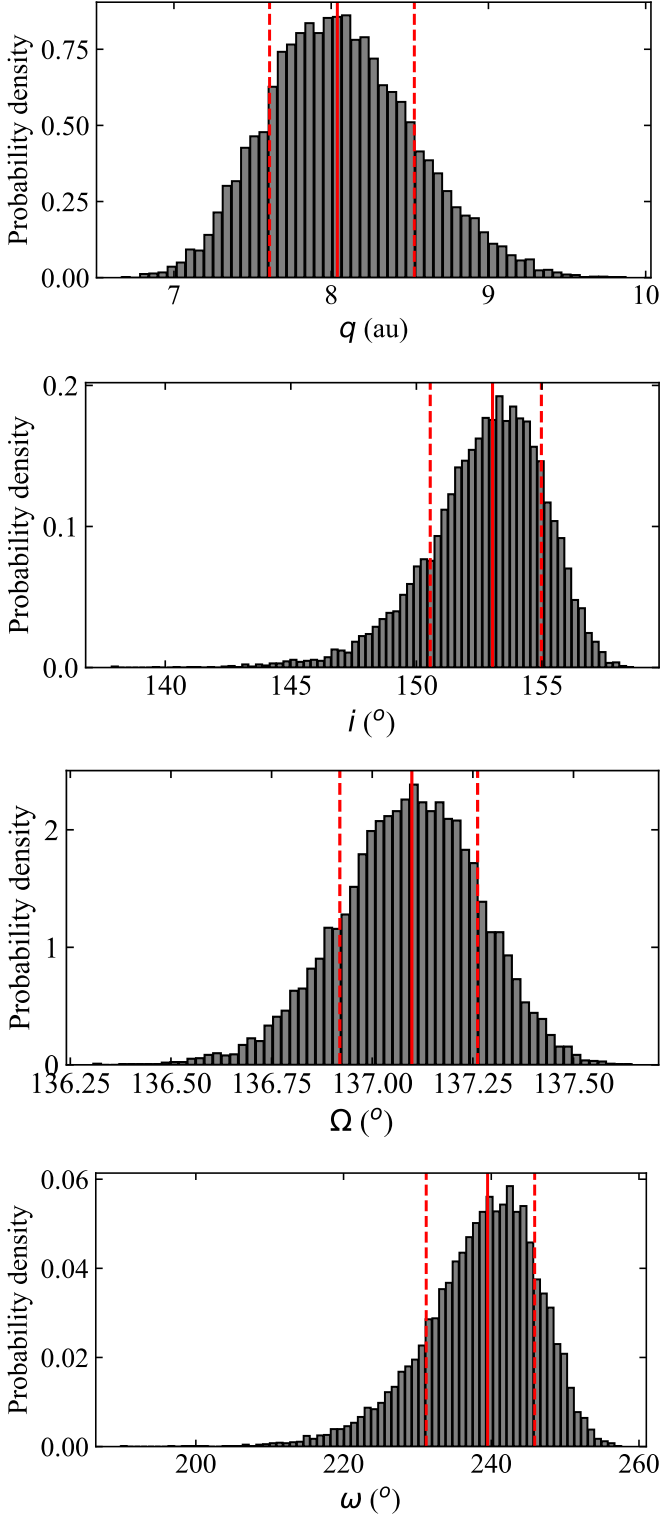


Fig. 6. Additional orbital elements of the pre-flyby orbit of C/2024 L5 (ATLAS). *Top panel:* Distribution of the computed pre-flyby peri-helion distance. *Second to top panel:* Orbital inclination. *Second to bottom panel:* Longitude of the ascending node. *Bottom panel:* Argument of perihelion. Median values are displayed as continuous red lines, 16th and 84th percentiles as dashed lines.

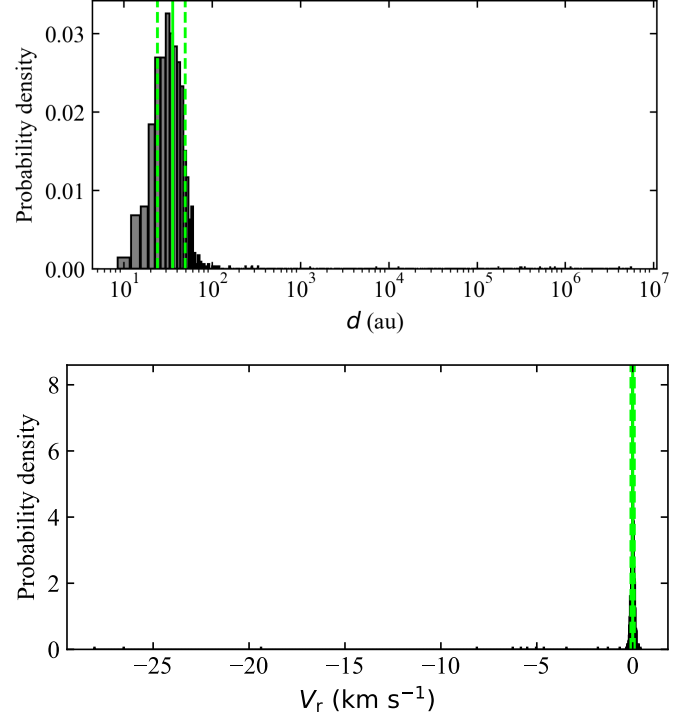


Fig. 7. Range of distance and range rate of C/2024 L5 (ATLAS), 1.0 Myr prior to its encounter with Saturn. *Top panel:* Distribution of distances at the end of the simulations, 36^{+14}_{-12} au. *Bottom panel:* Distribution of radial velocities at the end of the calculations, $0.00^{+0.08}_{-0.09}$ km s⁻¹. Distributions resulting from the evolution of 10^3 control orbits. The median is displayed as a continuous vertical green line, the 16th and 84th percentiles as dashed lines.

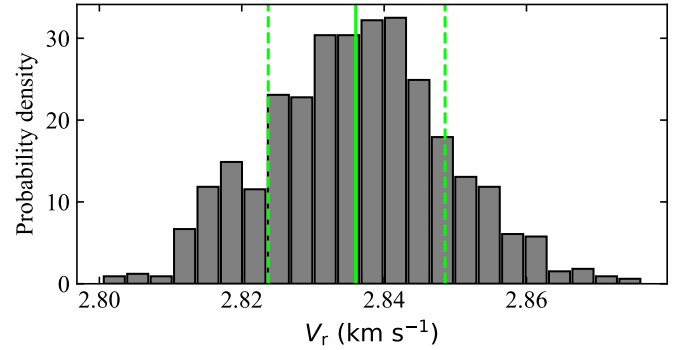


Fig. 8. Receding velocity of C/2024 L5 (ATLAS) after escaping the Solar System. Distribution resulting from the evolution of 10^3 control orbits for 1.0 Myr. The median is displayed as a continuous vertical green line, the 16th and 84th percentiles as dashed lines, $2.836^{+0.013}_{-0.012}$ km s⁻¹.